Reviews

Microfluidic Approaches for Protein Crystal Structure Analysis

Masatoshi MAEKI,*,† Hiroshi YAMAGUCHI,*** Manabu TOKESHI,* and Masaya MIYAZAKI**†**

*Division of Applied Chemistry, Faculty of Engineering, Hokkaido University, Kita 13 Nishi 8, Kita, Sapporo 060–8628, Japan
**Advanced Manufacturing Research Institute, National Institute of Advanced Industrial Science and Technology, 807-1 Shuku, Tosu, Saga 841-0052, Japan
***Liberal Arts Education Center, Aso Campus, Tokai University, Minami-Aso, Kumamoto 869–1404, Japan

This review summarizes two microfluidic-based protein crystallization methods, protein crystallization behavior in the microfluidic devices, and their applications for X-ray crystal structure analysis. Microfluidic devices provide many advantages for protein crystallography; they require small sample volumes, provide high-throughput screening, and allow control of the protein crystallization. A droplet-based protein crystallization method is a useful technique for high-throughput screening and the formation of a single crystal without any complicated device fabrication process. Well-based microfluidic platforms also enable effective protein crystallization. This review also summarizes the protein crystal growth behavior in microfluidic devices as, is known from viewpoints of theoretical and experimental approaches. Finally, we introduce applications of microfluidic devices for on-chip crystal structure analysis.

Keywords Microfluidic device, protein crystallization, protein crystallography, *in-situ* X-ray analysis

(Received August 25, 2015; Accepted October 6, 2015; Published January 10, 2016)

1 Introduction

Over the last few decades, protein crystallography has achieved outstanding progress through the development of automated robots, improved crystallization methods, new methodologies for crystal structure analysis, and improvements of synchrotron source facilities.[1–11] In addition, several preparation strategies for valuable protein samples, such as expressing, refolding, and purifying, have been established to perform protein crystallization experiments efficiently. Information on protein three-dimensional structures allows a structure-based drug design for cost-effective and highly efficient drug development.[12,13] Three-dimensional protein structure analysis consists of the following processes: protein sample preparation, protein crystallization, and X-ray crystal structure analysis.[14] First, the target protein preparation involves the expression and purification steps. To obtain the protein crystal, a high-purity

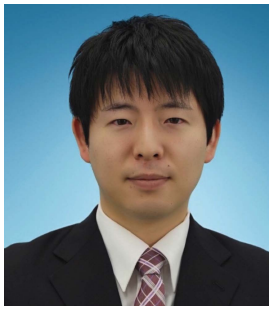

Masatoshi MAEKI received his Ph.D. degree in 2014 from Kyushu University. He worked at Hokkaido University as Research Fellow of the Japan Society for Promotion of Science (JSPS) (2014 – 2015) and as Assistant Professor of Division of Applied Chemistry (2015 –). He also worked at National Institute of Advanced Industrial Science and Technology (AIST) as Invited Researcher (2014 –). His current research interests are the development of microfluidic systems for analytical biochemistry.

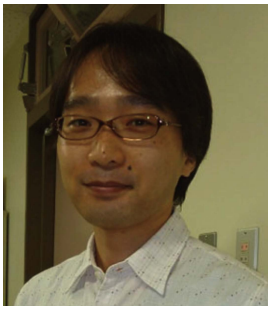

Hiroshi YAMAGUCHI obtained his Ph.D. in 2002 from Saga University. He worked as Visiting Fellow at NIH/NCI (2002 – 2007). He also worked at National Institute of Advanced Industrial Science and Technology as Research Fellow (2007 – 2011). Since 2011, he has been in Tokai University (Lecturer, 2011; Associate Professor, 2013 –) where he continues his research on applications of immobilized enzyme in analytical chemistry and enzymatic reaction using microfluidic chips for industries uses.

† To whom correspondence should be addressed.
E-mail: m.maeki@eng.hokudai.ac.jp (M. Maeki); m.miyazaki@aist.go.jp (M. Miyazaki)

protein sample is desirable. Then, the primary protein crystallization condition screening is carried out by manual pipetting or using an automated robot. When the appropriate conditions have been explored, the secondary condition screening, which optimizes the concentrations of protein, precipitant, and buffer, is conducted to obtain a high-quality crystal. Finally, the protein crystal structure is analyzed by using an in-house source X-ray diffraction system or a synchrotron facility.

The protein crystallization process is recognized as being a bottleneck in the protein structure determination process. This is because the protein crystallization condition screenings require large amounts of valuable protein samples, reagents and time. They are also labor-intensive. Automated dispensing robots (Mosquito®, Gryphon®, *etc.*) have been developed to facilitate the screening process, and to reduce the necessary amounts of protein sample and crystallization reagents.[1,15] Such equipment enables high-throughput screening for protein crystallization conditions, even though a hefty initial cost is one of the major disadvantages to be overcome. Moreover, the running cost is increased due to the trial-and-error approach for the protein crystallization condition screenings. Like in the protein crystallization, X-ray crystal structure analysis is also a complicated process. Protein crystals are fragile and have low mechanical strength, because they contain many water molecules in the crystal lattice. This property complicates the crystal structure analysis process, which includes protein crystal handling, cryoprotection, and X-ray analysis. For these reasons, protein crystallization and X-ray crystal structure analysis strongly depend on the skills of trained persons carrying out the work.

Microfluidic-based protein crystallization devices have been developed as an excellent and cost-effective apparatuses for protein crystallization and X-ray crystal structure analysis. For protein crystallization experiments, the use of microfluidic devices allows for small amounts of protein samples and crystallization reagents to be used, high-throughput screening for protein crystallization conditions to be achieved, and the nucleation and crystal growth behavior of the protein to be controlled.[16-25] Ismagilov's group reported on the potential of droplet-based microfluidics for protein crystallization condition screening.[17,38] Protein solution, precipitant solution, buffer solution, and additives (optional) were introduced at the inlet of the microfluidic device, followed by the formation of microdroplets of this mixture in oil. The crystallization conditions could be controlled by changing the flow rates of protein, precipitant, and buffer solutions. The volume of the microdroplets was also controllable by the flow-rate conditions. Hansen *et al.*[19] developed a well-based protein crystallization microfluidic device by free interface diffusion, which had 480 valves, they carried out 144 parallel crystallization experiments. The microfluidic devices also provide many advantages for X-ray crystal structure analysis, such as allowing on-chip cryoprotection and X-ray diffraction measurement.[26-31] Several microfluidic-based platforms, techniques, and approaches for protein crystallization have been studied. Notably, protein crystallization coupled with crystal structure analysis is the most significant methodology for novice researchers involved in protein crystallography.

In this article, we mainly review our microfluidic-based approaches for protein crystallization and their applications to X-ray crystal structure analysis. First, we summarize two microfluidic-based protein crystallization methods. Next, we describe the protein crystal growth behavior in microfluidic devices, as is known from viewpoints of theoretical and experimental approaches. Finally, we introduce applications of microfluidic devices for on-chip crystal structure analysis.

2 Droplet-based Protein Crystallization Method

For both conventional crystallization methods and microfluidic-based methods the principle of protein crystallization is based on classical crystallization theory.[32,33] In the case of the conventional crystallization methods (vapor diffusion, free interface diffusion, microbatch, and dialysis), a protein solution and a precipitant solution are mixed together to increase the supersaturation of the protein solution. Then, several microliters of the crystallization solution are placed on a crystallization plate, which is incubated at an appropriate temperature until protein crystals form in the solution. To obtain suitable protein crystals for X-ray analysis, a large number of conditions must be adjusted, such as the concentrations of the protein, precipitant, and the buffer, as well as the selection of appropriate additives, and the temperature. Microfluidic devices allow us to facilitate the protein crystallization condition screening with using just a small amount of the sample volume (several tens of nanoliters). Both droplet-based approaches and well-based approaches have been reported as platforms for microfluidic-based protein crystallization. Our two types of microfluidic devices for protein crystallization are shown in Fig. 1. Microfluidic devices are mainly made from polydimethylsiloxane (PDMS), glass, or polymer films. Droplet-based microfluidics is a fundamental research field in microfluidics. The microdroplets formed by

Manabu Tokeshi is a Professor at the Division of Applied Chemistry at Hokkaido University. He is also a Visiting Professor at ImPACT Research Center for Advanced Nanobiodevice at Nagoya University. He received his Ph.D. degree from Kyushu University in 1997. After a research fellow of the Japan Society for Promotion of Science at The University of Tokyo, he worked at Kanagawa Academy of Science and Technology as a research staff (1998 – 1999), a group subleader (1999 – 2003), and a group leader (2003 – 2004). He also worked at the Institute of Microchemistry Technology Co. Ltd. as President (2004 – 2005) and at Nagoya University as an Associate Professor (2005 – 2011). In 2011, he visited Karolinska Institutet as a Visiting Researcher and he joined the Hokkaido University as a Professor. His research interests are in the development of micro- and nano-systems for chemical, biochemical, and clinical applications.

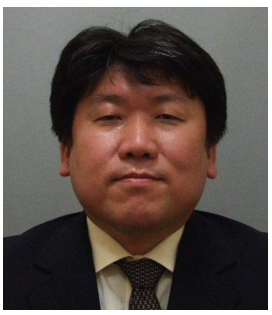

Masaya Miyazaki has a multidisciplinary background in the fields of analytical biochemistry, microfluidics, micro/nano-chemical devices, protein and peptide chemistry, and bioorganic chemistry. He graduated from Saga University with a B.Sc in bioorganic chemistry and pursued his Ph.D. at the same university, majoring in biochemistry. He was trained in the field of protein chemistry at Joslin Diabetes Center/Harvard Medical School, where he spent his postdoctoral training. After working at Japan Science and Technology Corporation (JST), he became a senior researcher at AIST. His current research interests include development of microfluidic reaction system and their application for analytical biochemistry including proteomic analysis.

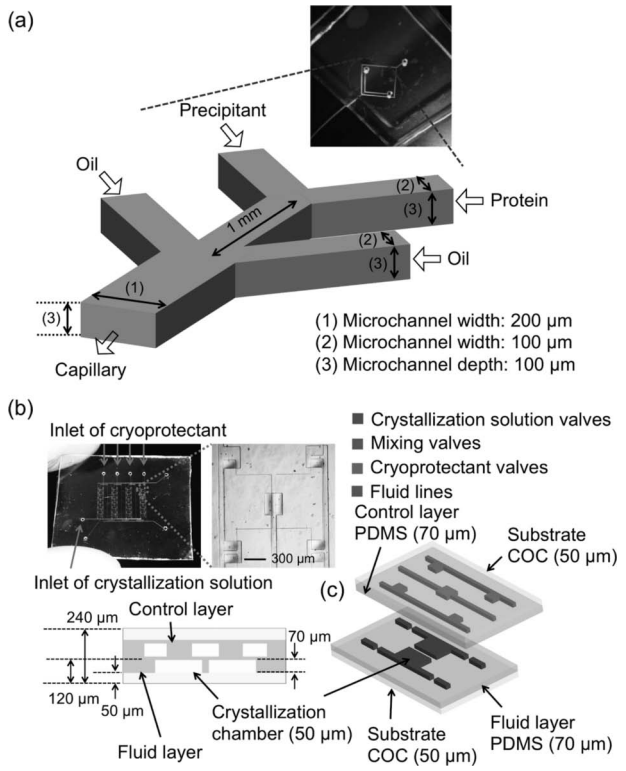

Fig. 1 (a) Photograph and schematic illustration of the microfluidic device for droplet-based protein crystallization. Reprinted from Ref. 25 with permission from Wiley. (b) Photograph of the microfluidic device for well-based protein crystallization. There are 24 crystallization chambers in one chip. The crystallization chamber dimensions are: 0.67 mm (width) × 0.75 mm (height) × 50 µm (depth). (c) 3D perspective view of the microfluidic device. Reprinted with permission from Ref. 26.

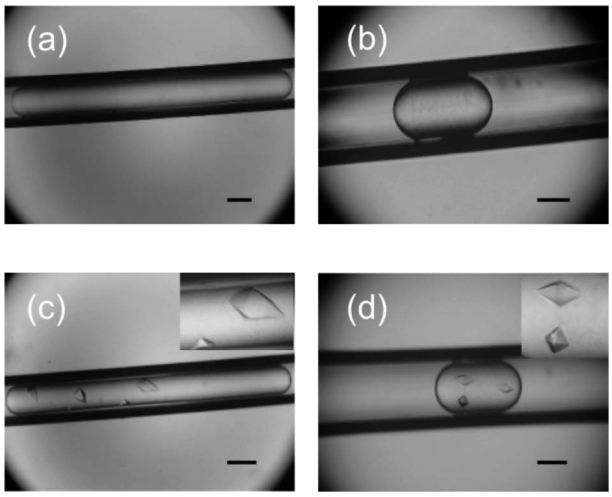

Fig. 2 Photograph of 50 nL volume droplets collected in the PFA capillary. (a) The capillary diameter is 200 µm. The droplet shape became elongated. (b) The capillary diameter is 360 µm. The droplet shape became elliptical. (c and d) Thaumatin crystal within a droplet after incubation for 24 h. Each scale bar represents 200 µm. Reprinted with permission from Ref. 24 with permission from the Chemical Society of Japan.

microfluidic devices have the following features: monodispersity, excellent reproducibility, high-throughput, and a volume on the pL to nL level.[33–37] Droplet-based protein crystallization by the vapor diffusion method was also reported as one application using interesting characteristics of microfluidics.[39] Microdroplets of protein and precipitant solution were alternately formed in the microfluidic device. Water molecules in the protein droplet could diffuse to the precipitant droplet *via* water-permeable oil.

We have demonstrated the droplet-based protein crystallization method for single crystal formation.[24,25,40,41] Single crystal formation is essential for protein crystallography to obtain a clear diffraction pattern by X-ray crystal structure analysis. When we can obtain one crystal in a microdroplet or a device, on-chip X-ray analysis is easily conducted without any complicated procedures. Typically, the microdroplet has different features from the macro-scale droplet. In particular, the small volume of the microdroplet and the large interface-to-volume ratio may affect the protein crystallization behavior. To investigate the effect of the microdroplet features on the protein crystallization, we demonstrated protein crystallizations in microdroplets that had different droplet volumes and shapes.[24] Thaumatin and lysozyme were used as model proteins, because they have been well investigated from the viewpoint of their crystallization behavior. In the case of thaumatin crystallization, the droplet volume and the shape affected the thaumatin crystallization behavior. Figure 2 shows photographs of 50 nL volume microdroplets formed by a microfluidic device. Droplets were collected in a PFA (perfluoroalkoxy alkane) capillary with an internal diameter of 200 or 360 µm. When a droplet was collected in a 200-µm capillary, its shape became elongated. On the other hand, a droplet in a 360-µm capillary was elliptically shaped, as shown in Fig. 2(b). After incubation for 24 h, we counted the number of thaumatin crystals that appeared in the droplet. As a result, the number of thaumatin crystals was increased with an increase of the droplet volume. We could obtain one thaumatin crystal within the small volume droplet regardless of the capillary diameter. In contrast, large-volume droplets (40 – 70 nL) produced a large number of thaumatin crystals. The number of thaumatin crystals formed in the droplet with a diameter of 360 µm was decreased compared to the droplet stored in the capillary with a diameter of 200 µm. Furthermore, in both diameter capillaries, getting a spherical droplet made it possible to obtain a single crystal formation. The thaumatin crystal growth was analyzed by using the Avrami equation.[42] The Avrami equation can be written as:

$$C = 1 - \exp(-kt^n)) \quad (1)$$

where C is the percentage of crystallization, k is the crystallization rate constant, t is time, and n is the Avrami exponent. The Avrami exponent indicates the mechanism of crystal growth. We found that thaumatin crystal growth was diffusion-controlled. In other words, the molecular diffusion of proteins to the surface of a nucleus or crystal was the limiting-step in droplet-based protein crystallization. Thus, in the elongated droplet (200 µm capillary) more crystals formed than in the elliptical droplet (360 µm capillary), even if the droplets had the same volume.

We also investigated the crystal growth rate of lysozyme within a microdroplet.[41] Our single crystal method is expected to be able to analyze protein crystal growth precisely, because the microdroplet does not contain any extra protein crystals. Lysozyme crystal growth was well analyzed for the (1 1 0) and the (1 0 1) crystal faces. Generally, the growth rate of both faces depends on the supersaturation condition. We crystallized lysozyme by changing the droplet volume and the concentration

of lysozyme. The (1 1 0) face grew faster than the (1 0 1) face under the high supersaturation condition. This result indicates that the crystal growth behavior in the microdroplet is almost the same as the conventional crystal growth behavior.

3 Well-based Protein Crystallization Method

Well-based microfluidic platforms provide many advantages for protein crystallization. Microfluidic device integrated valves can precisely control the protein crystallization conditions, although their fabrication process may be a little more complicated than that of droplet microfluidics systems. Ismagilov's group reported a SlipChip-based approach to demonstrate the multiplex screening of protein crystallization conditions.[18,43] The protein crystallization experiment using the SlipChip is composed of the following simple steps: loading of the protein sample and precipitants, slipping of the device (mixing), and crystallizing. To introduce reagents into the device and to mix them, no external equipment (syringe pump, vacuum pump) is required. The crystal structure of glutaryl-CoA dehydrogenase was determined by X-ray crystal structure analysis.

Kenis's group has demonstrated the applicability of the microfluidic device for membrane protein crystallization.[44] A structural determination of membrane proteins is strongly desired in the field of drug discovery. The microfluidic device and the lipidic cubic phase crystallization method were combined for membrane protein crystallization. The microfluidic device was fabricated from PDMS and the cyclic olefin copolymer (COC) by using standard photolithographic procedures. For the crystallization of a photosynthetic reaction center, a membrane protein from *Rhodobacter sphaeroides* was conducted using the microfluidic device. The protein solution was introduced into the microfluidic device *via* a vacuum pump, and was incubated for 4 – 12 h to obtain a protein-enriched mesophase. Protein crystals were formed in the mesophase during further incubation for several days. Then, the protein crystals were analyzed by on-chip X-ray analysis at room temperature, and the crystal structure was obtained to a resolution of 2.5 Å.

4 Protein Crystal Growth in Microfluidic Devices

Analysis of protein crystal growth behavior provides significant information for forming a high-diffraction quality protein crystal. We have analyzed protein crystallization behavior in the microdroplet by theoretical and experimental approaches.[25,40,45] Spherical microdroplets with different diameters (130, 200, 360, and 500 μm) were prepared to evaluate the effect of protein molecular diffusion on the crystallization behavior. When we used a small size droplet, one protein crystal formed in the droplet, as shown in Table 1. Described from the viewpoint of nucleation and crystal growth, protein molecules in the droplet diffuse to the nucleus, which is followed by crystal growth. Therefore, protein molecules around the crystal are consumed by the crystal growth and a protein concentration gradient forms in the droplet. Then, protein molecules are transported to the nucleus or crystal neighborhood by molecular diffusion. We defined the critical droplet size to obtain only one crystal within a microdroplet as follows:[40]

$$R_c = (6DC_0/q)^{1/2} \quad (2)$$

Table 1 Number of crystals observed per single droplet

Droplet diameter/μm	Number of crystals per droplet[a]
130	1.0 ± 0.2
200	1.2 ± 0.3
360	1.3 ± 0.5
500	2.1 ± 0.7

a. 100 – 200 droplets were observed for each droplet diameter size. The number of crystals is presented as the average ± standard deviation. Reprinted with permission from Ref. 40 with permission from the Royal Society of Chemistry.

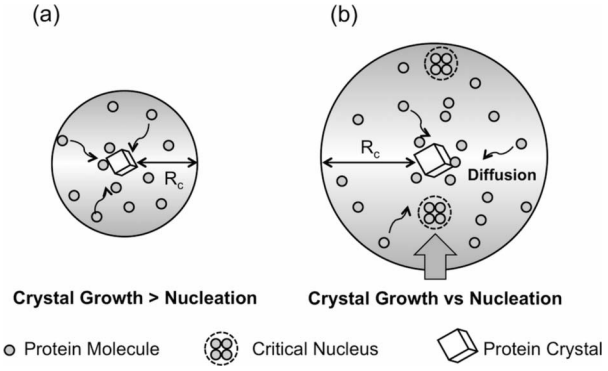

Fig. 3 Concept of the single crystallization method based on droplet microfluidics. (a) Droplet size < critical size (R_c). (b) Droplet size > R_c. The critical size was estimated from the diffusion coefficient, the initial concentration of protein, and the consumption rate of protein in solution. Reprinted with permission from Ref. 24.

where R_c is the critical droplet size as a radius, D is the diffusion coefficient of the protein molecule, C_0 is the initial concentration of protein in the droplet, and q is the consumption rate of the protein. Figure 3 shows a schematic illustration of the single crystal method based on the critical droplet size. To demonstrate the concept of single crystallization, we carried out crystallization experiments of lysozyme (14 kDa), thaumatin (22 kDa), glucose isomerase (170 kDa, 4 subunits), and ferritin (440 kDa, 24 subunits).[25] The estimated R_c values were 600, 600, 450, and 200 μm, for lysozyme, thaumatin, glucose isomerase, and ferritin, respectively. However, the actual critical size was expected to be smaller than the estimated critical size due to a consideration of the assumptions of Eq. (2). For the crystallization of lysozyme, thaumatin, and glucose isomerase, only one protein crystal formed in the droplet with a diameter smaller than 360 μm, even when the high concentration solution of protein was used. In contrast, the crystallization behavior of ferritin crystals was different from that of the other proteins. Figure 4 shows the distributions of ferritin crystals formed in the droplet. A slight increase of the precipitant concentration induced multiple nucleations of the ferritin crystal, and the distribution of the crystals was wider. These results suggest that the molecular diffusion of protein is equally as important as the protein crystallization conditions for single crystal formation.

We have also attempted to image protein crystal growth in a microdroplet by using confocal Raman microscopy.[45] Microdroplets containing appropriate concentrations of thaumatin and precipitant were prepared by using a microfluidic device, and were collected in a PFA capillary. The capillary was placed in the sample stage. We confirmed the presence of a Raman peak at 2937 cm^{-1}; this corresponds to the C–H stretching

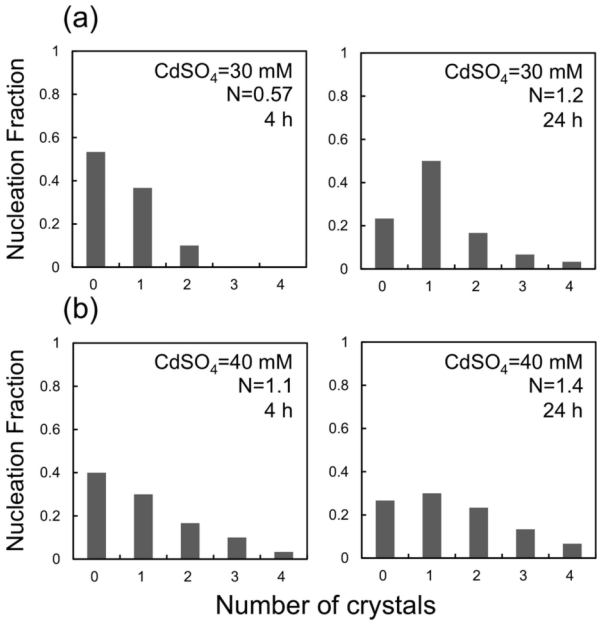

Fig. 4 Number of ferritin crystals in the 360 µm droplets. a) Precipitant concentration 30 mM $CdSO_4$. b) Precipitant concentration 40 mM $CdSO_4$. *N* is the mean number of ferritin crystals. Reprinted with permission from Ref. 24.

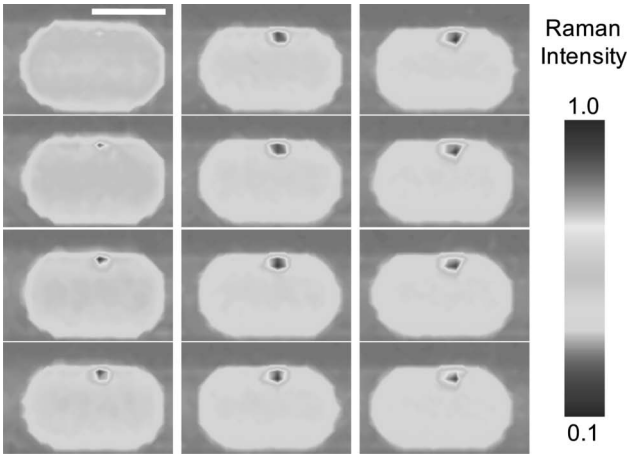

Fig. 5 Time evolution of the two-dimensional Raman mapping images, which indicates the change in the concentration of thaumatin in the droplet from nucleation and during the subsequent crystal growth processes. The images form a series moving from the upper left downward toward the lower right. Scale bar represents 200 µm. Reprinted with permission from Ref. 45 with permission from the Royal Society of Chemistry.

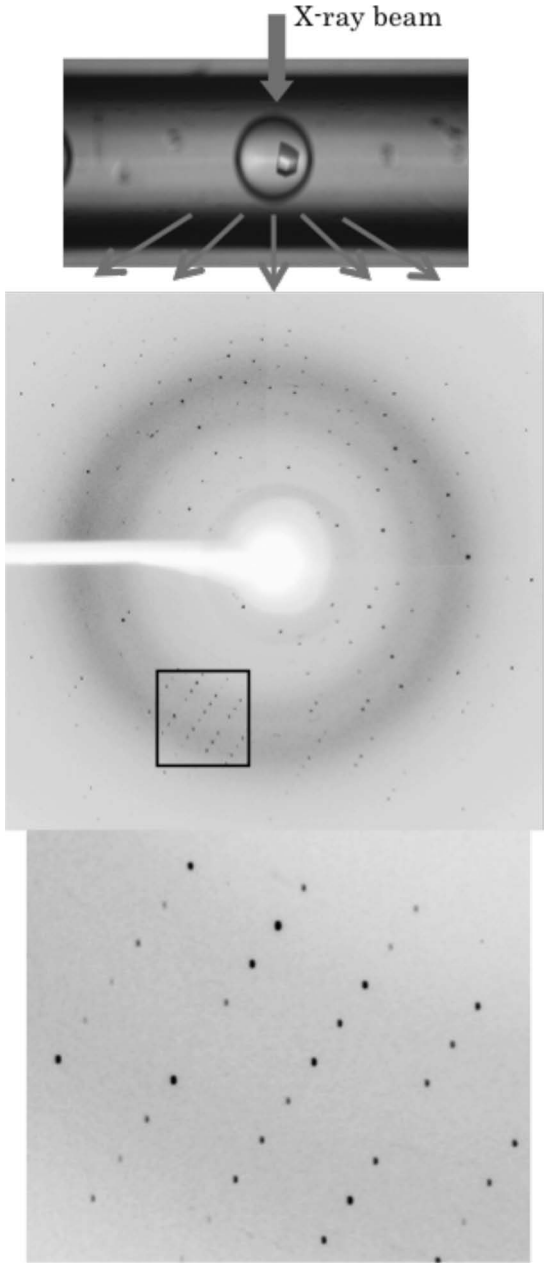

Fig. 6 Lysozyme crystal in a capillary (top), which could be directly subjected to X-ray diffraction. The obtained diffraction patterns (middle and bottom) were of sufficiently fine quality to generate crystal structure factors. Reprinted with permission from Ref. 27 with permission from The Japan Society for Analytical Chemistry.

vibration of the peptide backbone. This peak is best suited for obtaining mapping images by *in situ* Raman microscopy. The exposure time of the laser was adjusted to 5 s, although a longer laser beam exposure will increase the Raman intensity. Considering the large number of detection points (588 points) to obtain the Raman mapping image, these measurement conditions allowed us to detect the thaumatin crystallization behavior effectively. Figure 5 shows the time evolution of Raman mapping images during the crystal growth process at 64 min intervals. After nucleation (upper left), the Raman intensity of the droplet gradually decreased with time; conversely, that of the thaumatin crystal became stronger. The concentration of thaumatin around the crystal decreased after nucleation for 2 to 3 h. This suggests that thaumatin molecules around the crystal were incorporated into the crystal. Consequently, the concentration gradient formed and thaumatin molecules were transported to the neighborhood of the crystal. We consider that a coupling of droplet-based microfluidics and *in situ* Raman spectroscopic imaging offers a useful technique to analyze protein crystal growth without any complicated operations.

5 Application for X-ray Analysis

Generally, a protein crystal contains many water molecules in the crystal lattice. Therefore, the protein crystal is fragile, and requires careful and skilled handling for X-ray crystal structure analysis. Thus, a microfluidic approach, *i.e.* protein crystallization coupled with on-chip X-ray analysis, provides great advantages for protein crystal structure analysis. We demonstrated *in situ* X-ray diffraction measurements coupled with droplet-based protein crystallization, and examined the effect of the wall thickness and the material of the capillary used in the X-ray diffraction measurement.[27] Glass and PFA capillaries were used for *in situ* X-ray analysis. The thicknesses of the capillary walls were 10 and 80 μm for glass and PFA capillaries, respectively. In this *in situ* X-ray diffraction experiments, the protein crystal did not undergo the pretreatment called cryoprotection, which is generally used for X-ray analysis to prevent any degradation of the protein crystal. Therefore, 3 or 4 diffraction data were measured with 60 s exposure and 1° oscillation. Clear diffraction images were obtained by this method, as shown in Fig. 6, because our droplet-based single crystal method can produce only one protein crystal within a droplet. We determined the lattice constant, space group, and crystal system from several diffraction images, and found that the capillary wall thickness and material did not affect the determination of these crystallographic parameters.

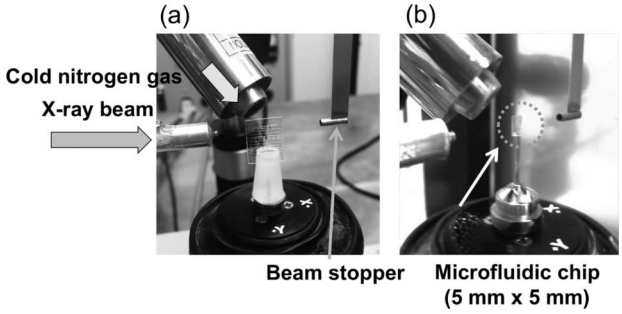

Fig. 7 Photographs of microfluidic devices in the on-chip X-ray diffraction experiment. (a) Photograph of the *in situ* X-ray diffraction experiment using a microfluidic device at 277 K. (b) Photograph of an optimized microfluidic device that was cut to a size of 5×5 mm^2. This microfluidic device was used for the X-ray diffraction experiment at 100 K. Reprinted with permission from Ref. 26.

For the past few years, large-scale synchrotron facilities have been developed. They make it possible to use a microcrystal for X-ray crystal structure analysis.[46,47] However, a high-intensity X-ray beam induces degradation of the protein crystal due to the formation of oxygen radicals in the protein crystal. To prevent degradation of the protein crystal, cryoprotection is a required and essential process. Typically, a protein crystal is soaked in a cryoprotectant (a solution for cryoprotection) by skilled manual handling for several minutes. Recently, we developed a new microfluidic platform that enables seamless experiments to be carried out from protein crystallization to X-ray crystal structure analysis.[26] Moreover, our microfluidic device was able to implement cryoprotection after protein crystallization without manual handling of the formed protein crystal. Also, we were able to carry out the X-ray diffraction analysis at 100 K to obtain a complete data set from one protein crystal; 90 diffraction data were measured with a 30-s exposure and 1° oscillation. Figure 7 shows photographs of the microfluidic devices in an on-chip X-ray diffraction experiment. A microfluidic device was optimized for X-ray analysis under the cryogenic condition (Fig. 7(b)). The effect of stepwise cryoprotection on the crystallographic data using the optimized microfluidic device was examined. Table 2 gives the crystallographic data results for lysozyme crystals with and without cryoprotection. The lysozyme crystal without cryoprotection was analyzed at 277 K (0 min). The resolution limit of a cryocooled lysozyme crystal was 1.6 Å, regardless of the cryoprotection procedure. On the other hand, the non-treated lysozyme crystal diffracted at a resolution limit of 1.8 Å, and the diffraction intensity from the lysozyme crystal gradually decreased with the duration of X-ray analysis. We confirmed the effect of stepwise cryoprotection by changing the mixing time of the cryoprotectant and the crystallization solution containing the lysozyme crystal. As a result, we found that short-step cryoprotection was able to effectively prevent degradation of the lysozyme due to osmotic shock by the cryoprotection procedure. Consequently, we consider that the combination of microfluidic-based approaches and synchrotron facilities can promote work on protein crystallization and X-ray crystal structure analysis.

6 Conclusions

In this review, we have summarized two microfluidic-based approaches for protein crystallization and their applications for X-ray analysis. Droplet-based protein crystallization allows us to promote crystallization experiments coupled with *in situ* X-ray analysis. Furthermore, we demonstrated the formation of

Table 2 Results of on-chip crystallographic data of lysozyme[a]

Space group	0 min (277 K)[b]	30 min (100 K)[c]	10 min (100 K)[c]	5 min (100 K)[c]
	$P4_32_12$	$P4_32_12$	$P4_32_12$	$P4_32_12$
Dimensions/Å	$a = b = 79.31$, $c = 37.86$	$a = b = 78.96$, $c = 37.03$	$a = b = 78.88$, $c = 37.06$	$a = b = 78.61$, $c = 37.03$
Resolution/Å	39.65 - 1.77 (1.86 - 1.77)	39.48 - 1.66 (1.75 - 1.66)	39.06 - 1.67 (1.76 - 1.67)	39.30 - 1.66 (1.75 - 1.66)
Mosaicity/deg	0.11	0.17	0.26	0.17
Completeness, %	93.1 (85.9)	99.2 (96.7)	96.6 (98.4)	97.9 (99.0)
R_{merge}, %	6.2 (81.8)	13.0 (51.0)	6.5 (53.4)	6.4 (27.6)
I/σ (I)	21.1 (3.2)	10.5 (3.9)	15.6 (3.4)	17.5 (7.0)

a. Values inside the parentheses represent the data of the outer shell. b. Data of the lysozyme crystal without cryoprotection at 277 K. c. Data of the cryocooled lysozyme crystal with different mixing times. The mixing time per one manipulation was changed as 5, 10, and 30 min. The total mixing time was fixed at 30 min. Reprinted from Ref. 26 with permission from the American Chemical Society.

a single crystal based on the critical droplet size, and obtained a high diffraction quality protein crystal. Well-based protein crystallization devices offer wide applications for protein crystallography. They were presented as a useful tool for novice researchers in protein crystallography. Microfluidic devices also enabled *in situ* measurement of crystal growth and on-chip X-ray crystal structure analysis. We believe that microfluidic-based approaches will be established as a fundamental analytical methodology for protein three-dimensional structural analysis.

7 Acknowledgements

A part of this work was supported by a Grant-in-Aid for JSPS Fellows 15J04557 (to M. Maeki).

8 References

1. R. C. Stevens, *Curr. Opin. Struct. Biol.*, **2000**, *10*, 558.
2. E. Abola, P. Kuhn, T. Earnest, and R. C. Stevens, *Nat. Struct. Biol.*, **2000**, *7*, 973.
3. T. Bergfors, *J. Struct. Biol.*, **2003**, 66.
4. M. Caffrey and V. Cherezov, *Nat. Protoc.*, **2009**, *4*, 706.
5. V. I. Strelov, I. P. Kuranova, B. G. Zakharov, and A. E. Voloshin, *Crystallogr. Rep.*, **2014**, *59*, 863.
6. G. Sazaki, E. Yoshida, H. Komatsu, T. Nakada, S. Miyashita, and K. Watanabe, *J. Cryst. Growth*, **1997**, *173*, 231.
7. V. I. Strelov, I. P. Kuranova, B. G. Zakharov, and A. E. Voloshin, *Crystallogr. Rep.*, **2014**, *59*, 863.
8. U. Weierstall, D. James, C. Wang, T. A. White, D. Wang, W. Liu, J. C. H. Spence, R. B. Doak, G. Nelson, P. Fromme, R. Fromme, I. Grotjohann, C. Kupitz, N. A. Zatsepin, H. Liu, S. Basu, D. Wacker, G. W. Han, V. Katritch, S. Boutet, M. Messerschmidt, G. J. Williams, J. E. Koglin, M. M. Seibert, M. Klinker, C. Gati, R. L. Shoeman, A. Barty, H. N. Chapman, R. A. Kirian, K. R. Beyerlein, R. C. Stevens, D. Li, S. T. A. Shah, N. Howe, M. Caffrey, and V. Cherezov, *Nat. Commun.*, **2014**, *5*, 3309.
9. G. Snell, C. Cork, R. Nordmeyer, E. Cornell, G. Meigs, D. Yegian, J. Jaklevic, J. Jin, R. C. Stevens, and T. Earnest, *Structure*, **2004**, *12*, 537.
10. A. E. Cohen, P. J. Ellis, M. D. Miller, A. M. Deacon, and R. P. Phizackerley, *J. Appl. Crystallogr.*, **2002**, *35*, 720.
11. G. Snell, C. Cork, R. Nordmeyer, E. Cornell, G. Meigs, D. Yegian, J. Jaklevic, J. Jin, R. C. Stevens, and T. Earnest, *Structure*, **2004**, *12*, 537.
12. T. L. Blundell, H. Jhoti, and C. Abell, *Nat. Rev. Drug Discovery*, **2002**, *1*, 45.
13. A. C. Cheng, R. G. Coleman, K. T. Smyth, Q. Cao, P. Soulard, D. R. Caffrey, A. C. Salzberg, and E. S. Huang, *Nat. Biotechnol.*, **2007**, *25*, 71.
14. N. E. Chayen and E. Saridakis, *Nat. Methods*, **2008**, *5*, 147.
15. J. Bard, K. Ercolani, K. Svenson, A. Olland, and W. Somers, *Methods*, **2004**, *34*, 329.
16. L. Li and R. F. Ismagilov, *Annu. Rev. Biophys.*, **2010**, *39*, 139.
17. B. Zheng, L. S. Roach, and R. F. Ismagilov, *J. Am. Chem. Soc.*, **2003**, *125*, 11170.
18. L. Li, W. Du, and R. F. Ismagilov, *J. Am. Chem. Soc.*, **2010**, *132*, 106.
19. C. L. Hansen, E. Skordalakes, J. M. Berger, and S. R. Quake, *Proc. Natl. Acad. Sci. U. S. A.*, **2002**, *99*, 16531.
20. A. M. Streets and S. R. Quake, *Phys. Rev. Lett.*, **2010**, *104*, 178102.
21. S. Talreja, S. L. Perry, S. Guha, V. Bhamidi, C. F. Zukoski, and P. J. A. Kenis, *J. Phys. Chem. B*, **2010**, *114*, 4432.
22. J. Shim, G. Cristobal, D. R. Link, T. Thorsen, and S. Fraden, *Cryst. Growth Des.*, **2009**, *9*, 1806.
23. M. IIdefonso, E. Revalor, P. Punniam, J. B. Salmon, N. Candoni, and S. Veesler, *J. Cryst. Growth*, **2012**, *342*, 9.
24. M. Maeki, H. Yamaguchi, K. Yamashita, H. Nakamura, M. Miyazaki, and H. Maeda, *Chem. Lett.*, **2011**, *40*, 825.
25. M. Maeki, Y. Teshima, S. Yoshizuka, H. Yamaguchi, K. Yamashita, and M. Miyazaki, *Chem. Eur. J.*, **2014**, *20*, 1049.
26. M. Maeki, A. S. Pawate, K. Yamashita, M. Kawamoto, M. Tokeshi, P. J. A. Kenis, and M. Miyazaki, *Anal. Chem.*, **2015**, *87*, 4194.
27. M. Maeki, S. Yoshizuka, H. Yamaguchi, M. Kawamoto, K. Yamashita, H. Nakamura, M. Miyazaki, and H. Maeda, *Anal. Sci.*, **2012**, *28*, 65.
28. L. Li, D. Mustafi, Q. Fu, V. Tereshko, D. L. Chen, J. D. Tice, and R. F. Ismagilov, *Proc. Natl. Acad. Sci. U. S. A.*, **2006**, *103*, 19243.
29. C. L. Hansen, S. Classen, J. M. Berger, and S. R. Quake, *J. Am. Chem. Soc.*, **2006**, *128*, 3142.
30. S. L. Perry, S. Guha, A. S. Pawate, A. Bhaskarla, V. Agarwal, S. K. Nair, and P. J. A. Kenis, *Lab Chip*, **2013**, *13*, 3183.
31. M. Heymann, A. Opthalage, J. L. Wierman, S. Akella, D. M. E. Szebenyi, S. M. Gruner, and S. Fraden, *IUCrJ*, **2014**, *1*, 349.
32. P. G. Vekilov, *Cryst. Growth Des.*, **2010**, *10*, 5007.
33. O. Galkin and P. G. Vekilov, *J. Am. Chem. Soc.*, **2000**, *122*, 156.
34. S-Y. Teh, R. Lin, L-H. Hung, and A. P. Lee, *Lab Chip*, **2008**, *8*, 198.
35. A. Huebner, M. Srisa-Art, D. Holt, C. Abell, F. Hollfelder, A. J. deMello, and J. B. Edel, *Chem. Commun.*, **2007**, 1218.
36. J. F. Edd, D. D. Carlo, K. J. Humphry, S. Köster, D. Irimia, D. A. Weitz, and M. Toner, *Lab Chip*, **2008**, *8*, 1262.
37. M. Fukuyama and A. Hibara, *Anal. Chem.*, **2015**, *87*, 3562.
38. D. L. Chen, C. J. Gerdts, and R. F. Ismagilov, *J. Am. Chem. Soc.*, **2005**, *127*, 9672.
39. B. Zheng, J. D. Tice, L. S. Roach, and R. F. Ismagilov, *Angew. Chem., Int. Ed.*, **2004**, *43*, 2508.
40. M. Maeki, H. Yamaguchi, K. Yamashita, H. Nakamura, M. Miyazaki, and H. Maeda, *Chem. Commun.*, **2012**, *48*, 5037.
41. H. Yamaguchi, M. Maeki, K. Yamashita, H. Nakamura, M. Miyazaki, and H. Maeda, *J. Biochem.*, **2013**, *153*, 39.
42. S. Chodankar, V. K. Aswal, J. Kohlbrecher, P. A. Hassan, and A. G. Wagh, *Physica B*, **2007**, *398*, 164.
43. L. Li, W. Du, and R. F. Ismagilov, *J. Am. Chem. Soc.*, **2010**, *132*, 112.
44. D. S. Khvostichnko, J. M. Schieferstein, A. S. Pawate, P. D. Laible, and P. J. A. Kenis, *Cryst. Growth Des.*, **2014**, *14*, 4886.
45. S. Nitahara, M. Maeki, H. Yamaguchi, K. Yamashita, M. Miyazaki, and H. Maeda, *Analyst*, **2012**, *137*, 5730.
46. K. Hirata, K. S. Itoh, N. Yano, S. Takemura, K. Kato, M. Hatanaka, K. Muramoto, T. Kawahara, T. Tsukahara, E. Yamashita, K. Tono, G. Ueno, T. Hikima, H. Murakami, Y. Inubushi, M. Yabashi, T. Ishikawa, M. Yamamoto, T. Ogura, H. Sugimoto, J. R. Shen, S. Yoshikawa, and H. Ago, *Nat. Methods*, **2014**, *11*, 734.
47. W. Liu, A. Ishchenko, and V. Cherezov, *Nat. Protoc.*, **2014**, *9*, 2123.